

Pulsed Thermographic System for Non-destructive Characterization of Biological Materials

A Design Project Report

**Presented to the School of Electrical and Computer Engineering of Cornell
University**

**in Partial Fulfillment of the Requirements for the Degree of
Master of Engineering, Electrical and Computer Engineering**

Submitted by

Guangxun Zhai

MEng Field Advisor: Yu Jiang

Degree Date: January 2024

Abstract

Master of Engineering Program

School of Electrical and Computer Engineering

Cornell University

Design Project Report

Project Title: Active Thermography System

Author: Guangxun Zhai

Abstract

This project report presents the development of a novel thermography-based method for non-destructive characterization of biological materials for agricultural applications. The report details the mechanical, electrical, and software design of the instrument, which includes data acquisition and analysis using computer vision and machine learning techniques. The results revealed correlations between organic tissue status and tissue responses to thermal simulations. Two cases studies were performed to prove the hypothesis and for developing a robust ML model for the identification. Future development includes the implementation of a calibration method to eliminate non-uniform heating radiation and the development of a more robust machine learning model to improve classification accuracy. Overall, this project demonstrates the feasibility and high accuracy of thermography for assessing crop health, which has the potential to revolutionize crop management practices and improve overall crop yields.

1 Executive Summary

An effective active thermography system is composed of two primary components: data acquisition from the hardware camera and data processing using computer vision (CV) and machine learning (ML) techniques to develop a model for identifying the live or dead state of a plant. In this project, the focus has been on developing an accurate and efficient method for data acquisition, to enable the collection of large volumes of data and facilitate the development of a robust model.

The project consists of various modules. The hardware component comprises a high-resolution thermal camera, metal structures for placing samples and fixing lamps and cameras, a USB switch that can receive signals from a PC and control the lamps, and two heating lamps. The software component includes a cooperative GUI that helps to collect data based on specific requirements, as well as various software programs for computer vision and machine learning.

The most significant contribution of this project is the development of a software GUI that integrates with the thermal camera's API and can be customized to suit specific project needs. This sophisticated software tool utilizes multi-threading and offers a wide range of camera functions and parameter changes. Following data acquisition via the GUI, CV segmentation is used to extract each sample and label them for training the ML model.

The data acquisition process encountered several challenges, which were gradually addressed during the two semesters of the project. However, some issues remain unresolved at present. One issue concerns a visual problem in the software GUI when loading 16-bit data. Although the final data is not affected, normalization of image data for CV2 streaming can introduce noise under certain conditions, which is difficult to resolve. The second issue relates to calibration after data acquisition. Because two heating lamps are manually used for the heating process, the thermal radiation may not be uniform due to variations in the lamps' positions, requiring calibration.

In conclusion, this project successfully developed a software GUI for data acquisition that enabled the collection of large volumes of data for training an ML model to identify the live or dead state of a plant. However, further work is necessary to address the remaining challenges and ensure the accuracy and robustness of the final model.

2 Introduction

Assessing the health of crops has always been a critical and complex task in the field of agriculture. Farmers constantly face challenges in effectively identifying the health conditions of their harvested food or crop plants. The ability to accurately determine the well-being of crops is of utmost importance as misidentifying their health conditions can have significant consequences. For farmers, false identification can directly impact the autumn harvest, leading to financial losses and a decline in productivity. Additionally, inaccurate identification methods can result in low-quality agricultural products entering the market, which adversely affects consumer trust and increases daily food expenses.

Moreover, recent studies have highlighted an increasing demand for high-quality food among consumers. As individuals become more health-conscious and aware of the impact of food on their well-being, the need for precise and efficient methods to evaluate the health of agricultural plants becomes even more significant. Fortunately, advancements in artificial intelligence and hardware development offer promising opportunities to address this global issue.

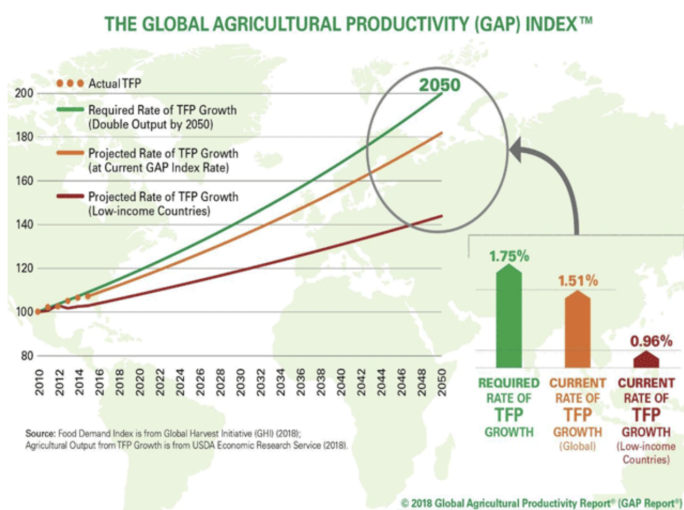


Figure 1: The 2018 Global Agricultural Productivity (GAP) Index. It outlines that our agriculture food production might not meet a more fast growing demand of it.
(Steensland, et al., 2018).

Currently, the most common methods used to identify the health of crops involve visual observation of the plant's surface or random sampling that requires cutting the crop apart to examine its internal condition. However, these approaches are time-consuming, subjective, and lack precision. Furthermore, they may cause unnecessary physical damage to the crops, leading to potential wastage of food resources. Another advanced potential approach would be using computed tomography (CT) scanning, however, the cost of using this method is prohibitive for most farmers and might even exceed their revenue.

To overcome these limitations, a more advanced and non-invasive solution involves using thermal

imaging techniques, specifically pulsed thermography, to assess the health status of crops. Pulsed thermography is an type of active thermography and has been widely applied to detect the quality variation between distinctive materials. (Maldague, et al., 1996, 2002). By capturing and analyzing the infrared radiation emitted by plants, thermography provides valuable insights into their physiological condition. This method allows for quick and non-destructive evaluations, making it an attractive alternative to traditional approaches.

In our research, we have developed an active thermography system that collects thermal data from crops and utilizes this data to identify their health condition. Different from other developed non-destructive quality evaluation (Wu, et al., 2013; He, et al., 2022), such as on fruit bruises (Kuzy, et al., 2018; Jiang, et al., 2016), which the assessment might be limited to the surface or shallow depth of the tissues. Our system might penetrate deeper and get a full picture information the plants' internal configuration. The system consists of three main components: data collection, data processing, and data analysis with the aid of a machine learning (ML) model. During the data acquisition, we first choose one specific type of crop, safely heat it for a while, and collect its thermostat variation during the heating and cooling period. The collected thermal data is processed and normalized to ensure accurate and reliable results. We also employ computer vision (CV) segmentation techniques to isolate individual crop samples, further enhancing the precision of the analysis.

The processed data is then fed into an ML model, which has been trained with condition tags, enabling it to classify and identify the health status of the crops. By utilizing the power of machine learning, we can achieve higher accuracy and efficiency in assessing crop health. Once the ML model demonstrates a high level of accuracy, it can be used to quickly identify the health conditions of other crops of the same type.

In addition to system development, we recognize the importance of integrating our solution into real-world applications and industrial production processes. By ensuring compatibility and adaptability to different contexts, our active thermography system can effectively contribute to the advancement of the agriculture industry. These efforts aim to bridge the gap between research and practical implementation, making our innovation accessible and beneficial to a wider audience.

Within our laboratory, we place significant emphasis on the continuous improvement of the system's performance, precision, and user-friendliness. We strive to refine its accuracy by conducting rigorous testing, data analysis, and validation processes. Simultaneously, we place great importance on optimizing the usability of the system, making it intuitive and straightforward for users to operate.

By adopting our thermography-based approach, we aim to revolutionize the identification of crop health by providing a cost-effective and efficient solution. The integration of artificial intelligence and hardware advancements into the agricultural sector holds great promise in improving crop quality and reducing financial losses for farmers. Additionally, consumers will benefit from increased access to high-quality agricultural products, leading to improved overall food security and affordability.

The overarching goal of our project was to offer an innovative and reliable method to assist humans in accurately identifying the health status of biological agricultural plants. Specific objectives included: first, we need to construct a robust software interface for collecting the data from raw plant samples; second, we are required to preprocess the data we retrieved (like calibration or segmentation); the last is to utilize statics and Machine Learning tool to analyze the final processed data and built a robust model for identification.

3 Design

3.1 System Design Graph

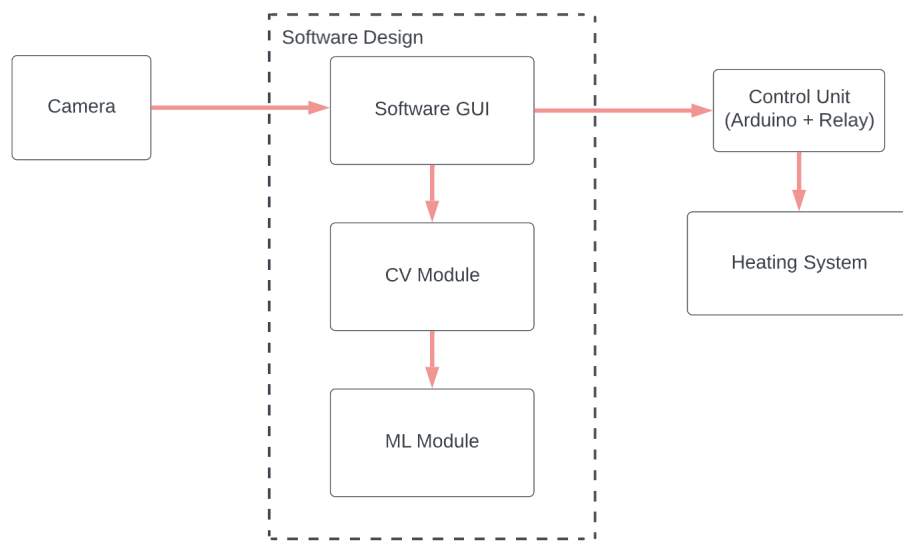


Figure 2: System Design Graph of our Pulsed Thermographic System

3.2 Mechanical Design

The mechanical design of our instrument was primarily handled by our undergraduate researcher, Alan Zayd Zoubi. The main structure of the instrument was created using 3D printing, which allowed for precise and customizable manufacturing. In the center of the instrument, we placed a black platform made from HPEC material, which has a high radiation emissivity. This ensures that the platform doesn't reflect too much thermal radiation, which could interfere with our data collection.

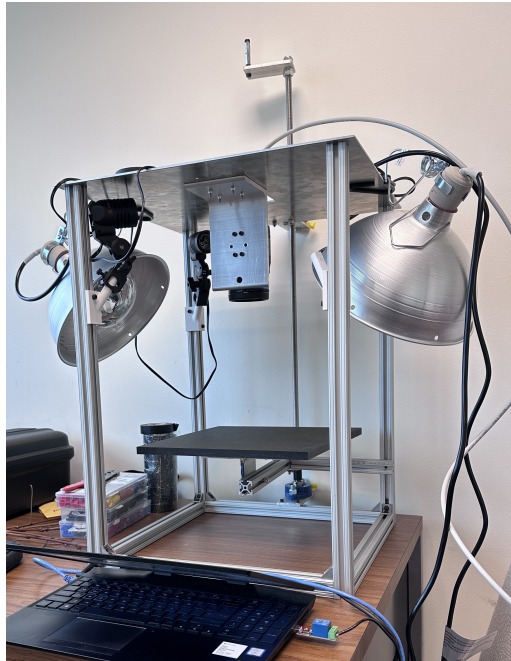


Figure 3: Physical Look of our Pulsed Thermographic System

The thermal camera (FLIR a700) is mounted on top of the instrument, and there are special mechanical parts beneath the platform that allow it to spin and move up and down, so we can adjust its position relative to the camera. Additionally, we installed two heating lamps to provide customized heating. These lamps are carefully wired to our computing unit to ensure safety and functionality.



Figure 4: Thermal Camera (FLIR a700)

3.3 Electrical Design

The electrical design of our instrument is centered around the wiring that connects the lamps to our computing unit. Each lamp contains a 250W bulb, and we can have up to four lamps in total. The lamps use US outlets with a voltage of 120V, and the relay switch we use has a current capacity of 10A. To calculate the maximum current that will go through our circuit, we used the formula $4 \times 250 / 120 = 8.33A$. We chose to use 10 AWG wires for the main wiring, as this wire size can safely handle the current load.

For our USB relay module, we firstly tested on the srd-05vdc-sl-c model but eventually selected IOT Relay II for higher current/voltage capacity, convenience and safety. To connect to a traditional relay module and use it to control the lamps on/off, we need to cut the positive wire to a power stripe and connect both ends to the NC and COM pins of the relay. However, this IOT relay II contains 4 outlets so that we don't need to do the cut and wire work of a power stripe. We just connected it to an Arduino and connected Arduino to our PC so that we could use our computer to send control signal to the Arduino and to the relay module and eventually to the heating system.



Figure 5: IOT Relay II

3.4 Software Design

Our software design focused primarily on two key areas: data acquisition and data analysis. For data acquisition, we opted to use the PySpin dependency to integrate our software program with the FLIR thermal camera hardware. FLIR offers two SDK options - in C++ or Python - and we ultimately chose Python for the project. However, we encountered issues with dependency installation, specifically with the Spinnaker SDK, which has strict requirements for the Python version and may vary across different operating systems. After testing on Linux, MacOS, and Windows, we ultimately chose Windows as our final development OS due to issues with Ethernet connectivity on other platforms. The decision made here was mostly based on its ease of use, flexibility, and faster development cycle, which allowed us to make adjustments more quickly and efficiently to ensure that we could fulfill all the required features.

In the software level, to acquire data from the camera, I first had to initialize the FLIR camera system and retrieve a list of available cameras. For each camera found, the software then configures the camera settings, including pixel format, IR format, and acquisition mode. It retrieves calibration details and calculates various parameters based on the chosen IR format, starts image acquisition, and processes the images while the `_run_flag` is True. The processed image frames are then emitted as signals for use in the PyQt application, and the acquired data is saved in a .npy file while the parameters are written in a .cfg file. If an error occurs during image acquisition, the program prints the error and stops the acquisition, and after the acquisition is stopped, it deinitializes and releases the camera resources.

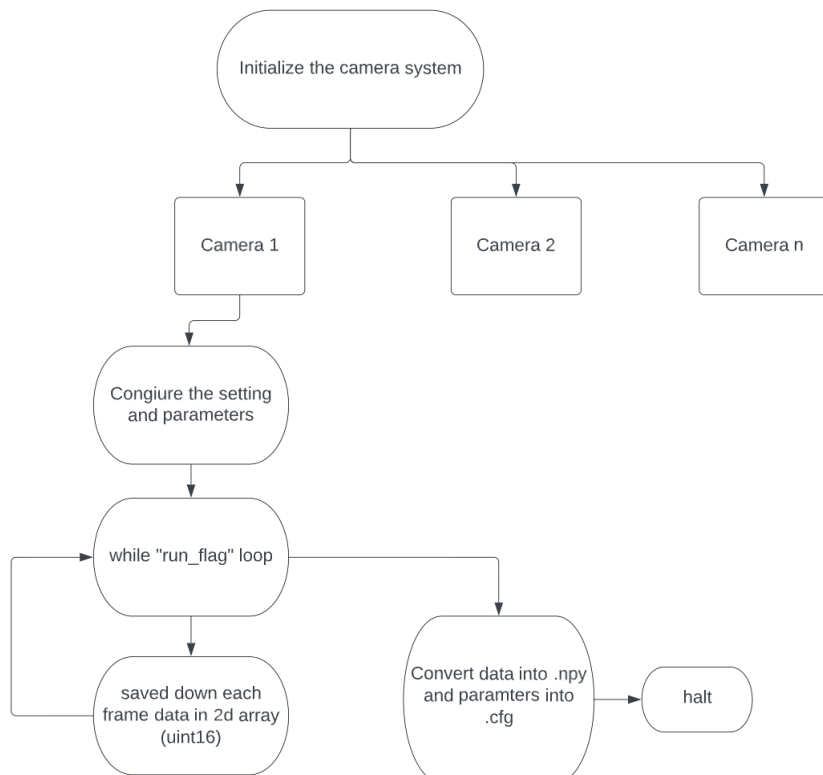


Figure 6: Control Flow Graph for the Data Acquisition

3.4.1 Software GUI

After completing the logic for data acquisition, we realized that a Python script alone would not suffice and that a GUI was necessary to view the camera's field of view during data acquisition and access additional camera features such as auto-focus, changing data saving name/path, adjusting parameters, etc. To address this, I used the pyQt5 package to build a GUI, with a separate thread for data acquisition to run independently of other processes. Three threads were built in total: one for informing the user that no input could be placed, one for streaming video, and the DAQ thread for data acquisition. I added various buttons and boxes to enable different functions that could be used with the camera. The GUI development was the most critical part of our software solution for the research project, and it took up most of our development time to make it sufficient and stable.

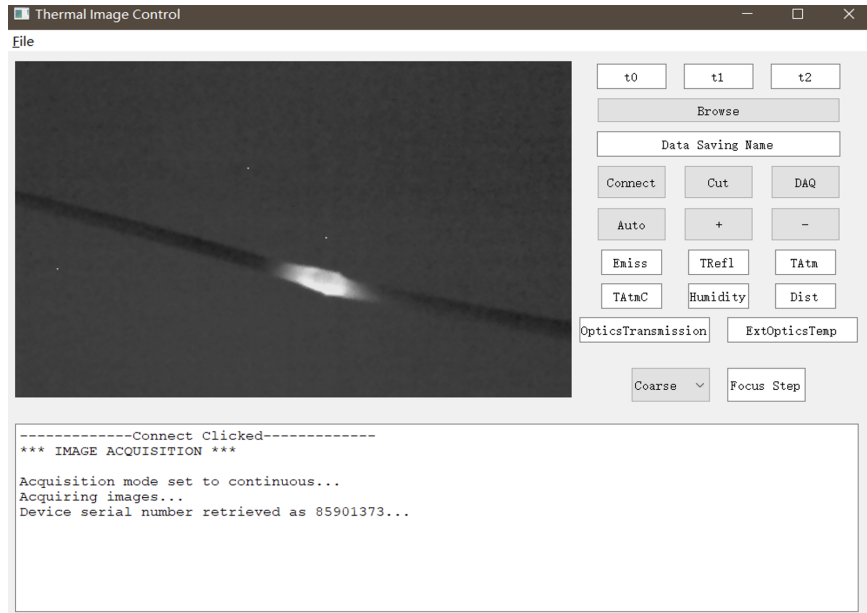


Figure 7: Basic software GUI in the streaming thread.

(Here I have just touched the grape bud to warm its up, so could see the bud part is whiter than other places since it generally has a higher temperature).

Features in the GUI:

- The camera image can be streamed in a separate window.
- There are three time boxes to set the data collection time for the DAQ. "t0" is for turning on the heating, "t1" is for turning it down, and "t2" is for ending the DAQ.
- The "Browse" button opens a window to allow the user to browse their PC storage and select a folder to save the data files. The text field next to it is used to set the image data filename.
- There are three buttons named "Connect", "Cut", and "DAQ" corresponding to the three threads in the program. The GUI starts with the "halt" thread, which displays no image. Pressing "Connect" initializes the system and connects to the camera, while "DAQ" activates the

data acquisition mode. The "Cut" button can be used to stop the camera at any time.

- The next row of buttons is for the camera's focusing method. "Auto" lets the camera perform an autofocus based on the focus method defined at the bottom, while "+" and "-" adjust the focus by the step value defined below.
- The next three rows of text boxes allow the user to change the environmental parameters used to compute the thermal data. Default values are provided, but they can be adjusted for more accurate data.
- The "Coarse" option is available for the focusing method, with an alternative option of "Fine".
- The "Focus Step" field is an integer value that determines the amount by which the focus changes when pressing "+" or "-".
- Finally, at the bottom of the GUI, there is a large text box that displays the terminal output. This is useful for monitoring the system as all terminal texts are printed here while the program is running.

3.4.2 CV Module

After completing the data acquisition, I developed a computer vision technique to extract thermal data for each seed sample, while excluding the background. The process involved finding a contrast frame, manually thresholding to segment the samples, recording their coordinate positions, calculating the mean and standard deviation for each seed with changing time, plotting the statistics, and saving them to a CSV file.

This approach allowed us to accurately identify changes in thermal activity within the seeds, which helped to monitor and evaluate the platform's efficacy with precision. By segmenting the image data and extracting the thermal data, we were able to determine the changes in thermal activity of each seed sample with high accuracy. Overall, this method provided us with a comprehensive understanding of the system's performance and helped us to make informed decisions based on the data.

Input frame

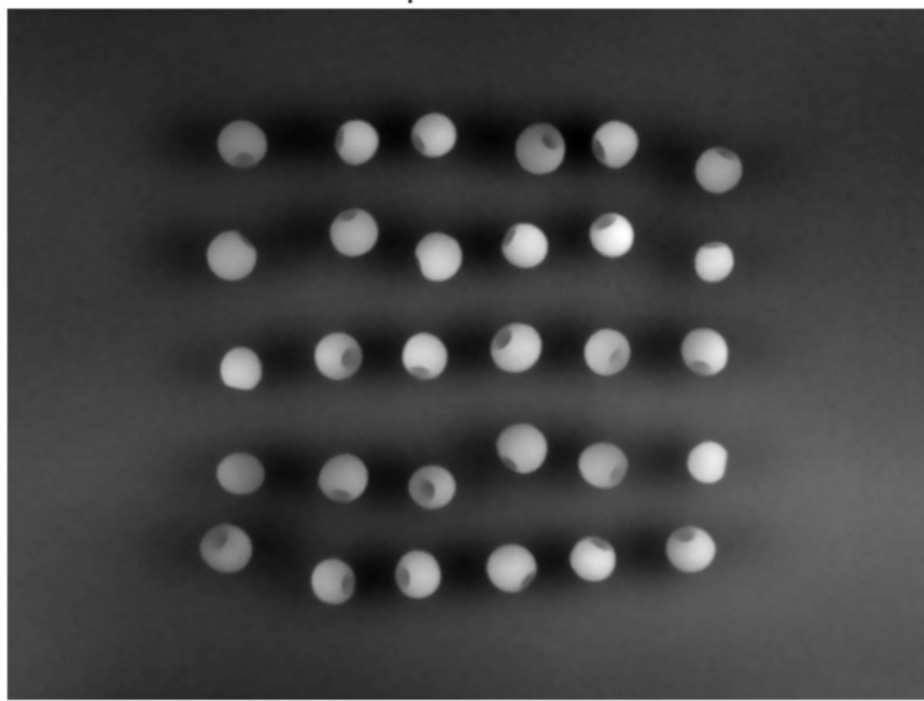


Figure 8: input frame before applying CV segmentation.

Thresholded image

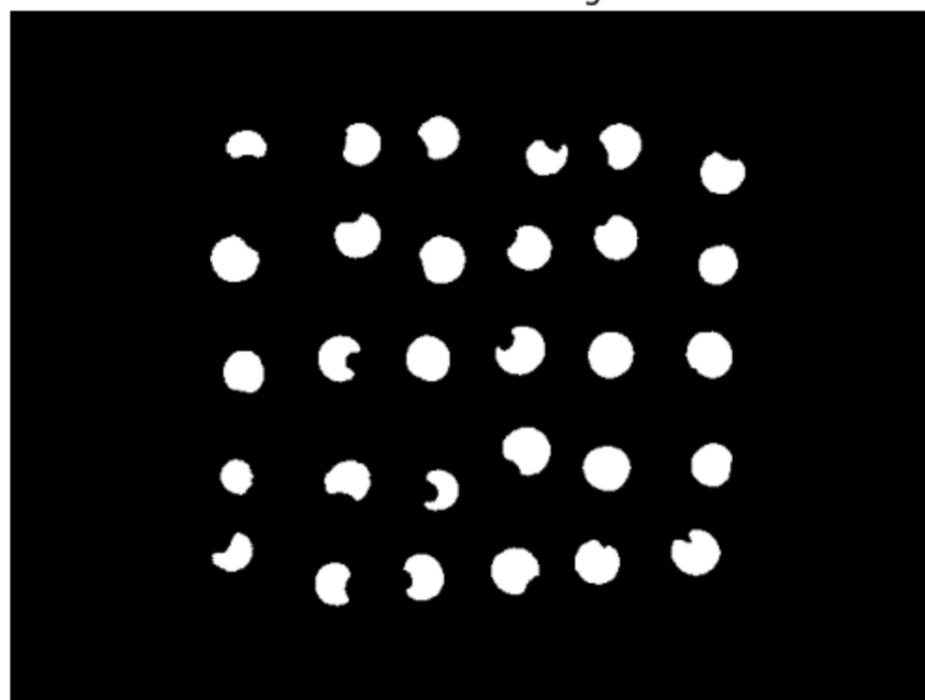


Figure 9: output frame after applying CV segmentation (threshold).

3.4.3 ML Module

For building our machine learning (ML) model and analyzing the results, we used Weka. We selected Weka for its efficiency, which was necessary to work with hundreds of data points and get a result fast and accurately. We plan to include calibration methods in the data collection to standardize the thermal data for the platform. However, for now, we only aim to test the data quickly to determine if we are moving in the right direction.

Overall, the software design project was a challenging but rewarding experience that required a combination of skills in programming, computer vision, and machine learning. The acquisition and analysis of thermal data was complex, and we faced multiple challenges and obstacles. Nevertheless, we successfully developed a robust and effective software solution that met all our research objectives. In the future, we plan to further enhance the software by adding more advanced features, improving the accuracy of the machine learning models, and expanding the scope of the project to other areas of research.

4 Case Studies

Two cases studies are conducted using our developed active pulsed thermographic system. One is on the grape buds, and another is one crop seeds.

4.1 Grape Bud Detection

4.1.1 Plant Materials

A total of 40 grapevine canes were randomly gathered from commercial vineyards in Geneva, New York, USA, comprising 5 representative cultivars:

- Gewurztraminer (*Vitis vinifera* L.).
- Merlot (*V. vinifera* L.).
- Cayuga White (*Vitis* sp. Hybrid).
- Noiret (*Vitis* sp. Hybrid).
- Concord (*V. labrusca* hybrid).

Eight replicate canes were selected from each cultivar. The canes were divided equally into two treatments: 1) natural cold damage and 2) supplemental freezing treatment (-17 °C for 24 hours following field collection) to guarantee all buds sustained damage. These two treatments would furnish ample samples with varying mortality statuses for subsequent analyses in this study.

4.1.2 Data Acquisition and Analysis

Data acquisition - Five grape buds on each cane were imaged using the custom-developed active thermographic system, with the thermal stimulation configured for 1 second prior to heating, 5 seconds of heating stimulation, and 10 seconds of cooling. This was equivalent to 480 frames in this study (thermal camera was set to 30 frames per second for 16 seconds). To minimize potential differences due to non-uniform heating stimulation among samples, only a single bud was placed at the center of the sample holder (and thus the image center). This process resulted in a dataset of 200 thermal image sequences (4 replicates for each of the 2 treatments across 5 cultivars).

Following image acquisition, all bud samples were manually sliced and examined to identify any potential damage (e.g., cold damage and missing buds) to the buds.

Image analysis – For each thermal image sequence, the image frame exhibiting the maximum heating effect (the 180th image frame) was presented to a human evaluator who selected the bud's center. A region of interest (ROI) was subsequently generated, featuring the selected center and a predefined radius of 5 pixels, to extract the thermal response curve for that particular bud.

Statistical analysis – A multivariate analysis of variance (MANOVA) was conducted to test for statistical differences between buds with varying mortality statuses, in order to assess the feasibility of using an active thermographic system for determining grape bud mortality. All analyses were performed in R, with a significance level of 0.05.

4.1.3 Results and Discussions

Significant differences in thermal responsive curves between healthy and damaged grape buds.

In general, a significant difference was observed in the thermal response curves between damaged and healthy bud samples (Figure 10A). During the idle period (the first 30 frames), the thermal radiation of damaged and healthy buds did not exhibit a significant difference, indicating their comparable initial status. As the heating stimulation commenced (from the 31st frame), the thermal radiation of healthy buds increased considerably more rapidly than that of damaged buds, resulting in a higher maximum thermal radiation at the 180th frame. Once the heating stimulation ceased (from the 181st frame), the thermal radiation of both types of buds began to cool down. Since the damaged buds had a lower maximum thermal radiation, their thermal radiation returned to the initial status more quickly. Conversely, the thermal radiation of healthy buds decreased at a slower pace and concluded at an intensity higher than the initial status. This suggested that a longer cooling period would be necessary for healthy buds to fully cool off. MANOVA tests demonstrated a statistical difference between damaged and healthy buds, validating the feasibility of using the extracted thermal response curves to distinguish bud mortality status.

Thermal responsive curves showed differences among cultivars

While the overall differences between damaged and healthy buds were significant, these differences exhibited variations among the five cultivars used in this study (Figure 10B). Cayuga White displayed the most robust thermal radiation of healthy buds during heating stimulation and the largest difference between damaged and healthy buds. This pattern was also observed for Gewurztraminer, Merlot, and Noiret, albeit with a relatively weaker thermal radiation of healthy buds and a smaller difference between damaged and healthy buds. In contrast, Concord demonstrated a considerably smaller difference between damaged and healthy buds. This was primarily due to the high thermal radiation intensity around the petiole scars on canes near the buds. These scars consistently exhibited high thermal radiation, which influenced the thermal radiation intensity of both surrounding buds and woody tissues, thereby reducing the difference between damaged and healthy buds. This factor could pose certain challenges in differentiating bud mortality status in practical applications

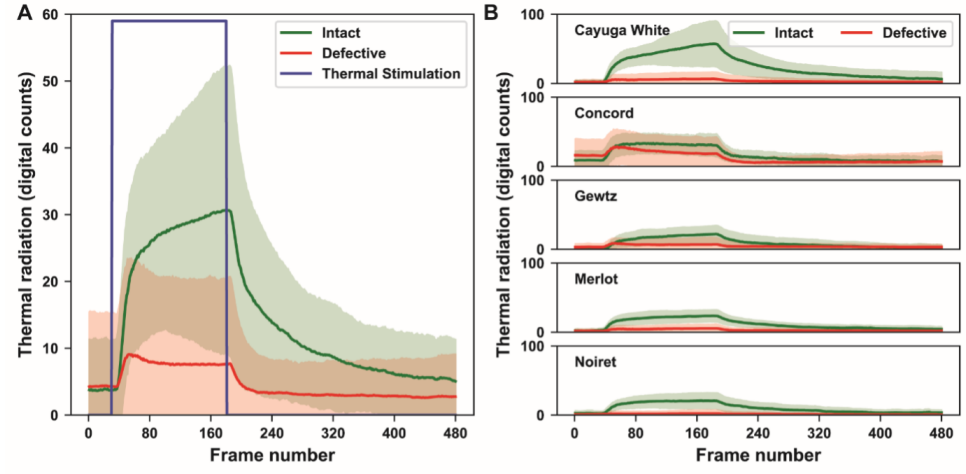


Figure 10: (A) Mean thermal responsive curves (solid lines) with standard deviation (shaded regions) of all samples with extracted thermal images for damaged (red line) and healthy (green) samples along with the thermal stimulation pulse curve (blue line); (B) Mean thermal responsive curves with standard deviation of samples of each cultivar for damaged and healthy samples.

4.2 Seed Detection

4.2.1 Plant Materials

120 crop seeds were selected to be used in this experiment, which contains half of them could be observed clear damaged on the surface of the seeds, and another half of them look well from outside.

4.2.2 Data Acquisition and Analysis

Data acquisition - The thermal stimulation is configured for 1 second prior to heating, 10 seconds of heating stimulation, and 19 seconds of cooling. This was equivalent to 900 frames in this study (thermal camera was set to 30 frames per second for 30 seconds). Data was also collected from different layouts and combinations of seed samples, and analyzed the results using computer vision and machine learning techniques.

To be more specific, I conducted four major treatments, each consisting of 30 seed samples arranged in 5 rows and 6 columns on the platform. The first treatment included 30 healthy seeds, while the second treatment included 30 unhealthy seeds with bug holes. The third treatment consisted of half columns of healthy seeds and the other half of unhealthy seeds. In the last treatment, I duplicated the third treatment, but I switched the positions of the two groups to eliminate the influence of non-uniform heating radiation. (A more detailed and direct view is shown in Figure 8).

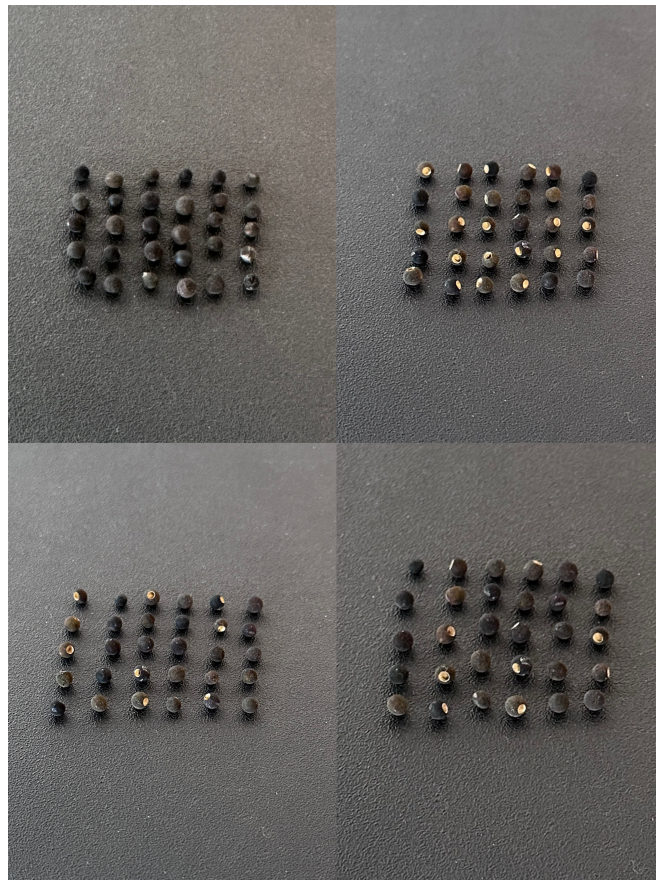


**Figure 11: Treatment 1 of 30 healthy seeds (top left);
Treatment 2 of 30 unhealthy seeds (top right);
Treatment 3&4 of 15 healthy and 15 unhealthy seeds (bottom two).**

Image analysis - Using the CV segmentation, I analyzed the thermal activity of the four treatments and plotted their mean values with standard deviation. To compare the behaviors of healthy and unhealthy seed samples, I combined the data from treatment 1 and treatment 2 on a single plot so as to clearer observe the difference between the seeds in opposite health status.

Once I collected the mean thermal data versus time for all 120 seeds, I labeled each seed and used Weka for machine learning analysis. I chose the J48 and RandomForest decision tree models since we only had two classes of data. While there is still room for improvement, the initial results have already provided evidence of the efficacy of our project.

4.2.3 Results and Discussions

Significant differences in thermal responsive curves of seeds in damaged and undamaged conditions.

Based on our experiments, we observed a noticeable correlation between a plant's viability and its temperature fluctuations. In particular, non-viable seeds have a higher quantity of air within their internal composition, which causes them to dissipate thermal energy more quickly. This finding is

significant as it provides insights into the thermal behavior of seed samples and can help inform future research in this area.

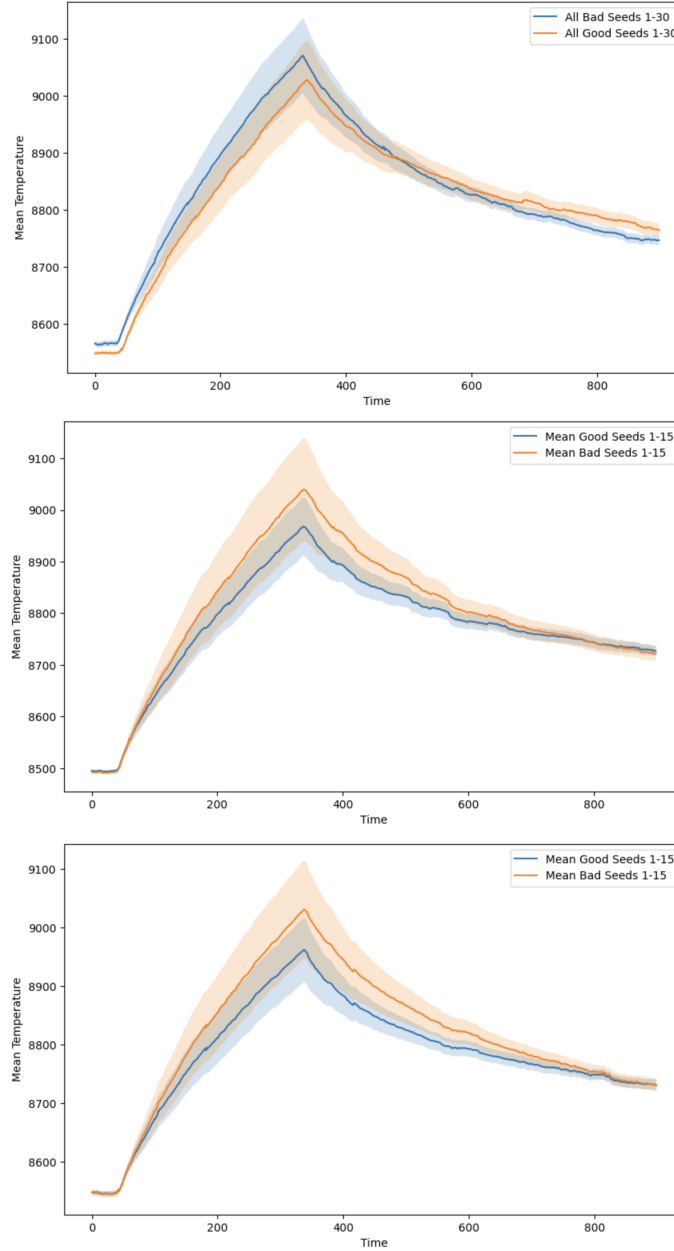


Figure 12: From top to bottom: Treatment 1&2; Treatment 3; Treatment 4. The curve is the mean thermal value of one type of seeds variation through time, and the shaded color is for the STD.

ML Model with moderate accuracy. From the experiment, our data contained 120 instances, which were randomly split into a training set and a testing set. The J48 algorithm achieved a classification accuracy of 76.67%, correctly classifying 92 instances and misclassifying 28 instances. The Random Forest algorithm performed slightly better, achieving a classification accuracy of 83.33%, with 100 instances classified correctly and 20 misclassified.

The Kappa statistic was used to evaluate the agreement between the actual and predicted class labels, with a value of 0.5333 for J48 and 0.6667 for Random Forest. These values indicate a moderate agreement between the actual and predicted class labels for both algorithms.

The mean absolute error and root mean squared error were used to evaluate the error of the models. For J48, the mean absolute error was 0.2354, and the root mean squared error was 0.4632. For Random Forest, the mean absolute error was 0.2463, and the root mean squared error was 0.3428.

The confusion matrix provides a summary of the classification results, showing the number of instances classified correctly and incorrectly for each class. For J48, 46 instances of the bad class were correctly classified, and 14 were misclassified as good. Similarly, 46 instances of the good class were correctly classified, and 14 were misclassified as bad. For Random Forest, 51 instances of the bad class were correctly classified, and 9 were misclassified as good. Likewise, 49 instances of the good class were correctly classified, and 11 were misclassified as bad.

The detailed accuracy by class provides further insight into the performance of the models for each class. For J48, the true positive rate, false positive rate, precision, recall, and F-measure were all 0.767 for both the bad and good classes. The Matthews correlation coefficient (MCC) was 0.533 for both classes. For Random Forest, the true positive rate, false positive rate, precision, recall, and F-measure were 0.850 and 0.817 for the bad and good classes, respectively. The MCC was 0.667 for both classes.

In conclusion, both the J48 and Random Forest algorithms were able to classify instances into the two classes with moderate accuracy. The Random Forest algorithm performed slightly better than J48, with a classification accuracy of 83.33% compared to 76.67%. However, both algorithms produced similar results in terms of the Kappa statistic and the detailed accuracy by class. These results indicate that the Random Forest algorithm may be a more suitable choice for this data set, but further experimentation and evaluation may be necessary to determine the optimal algorithm for this classification problem.

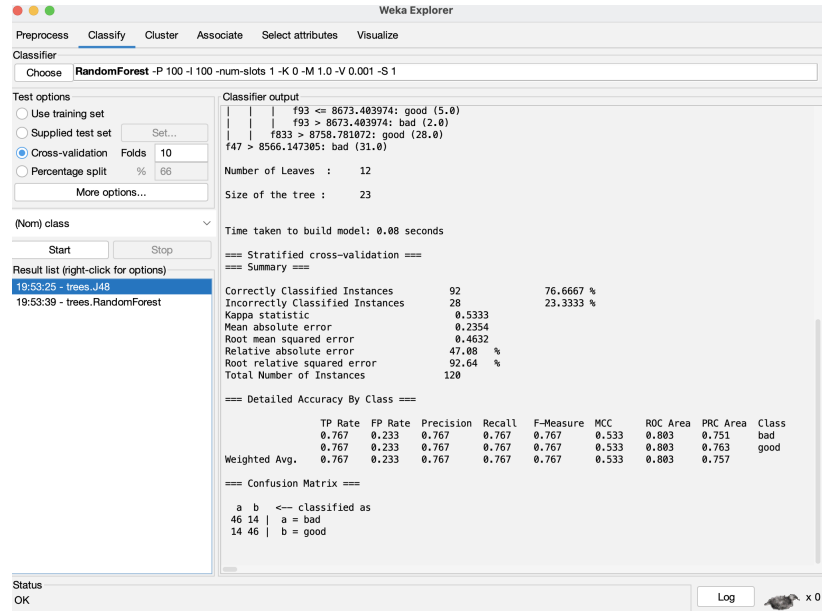


Figure 13: Weka Result using J48 model

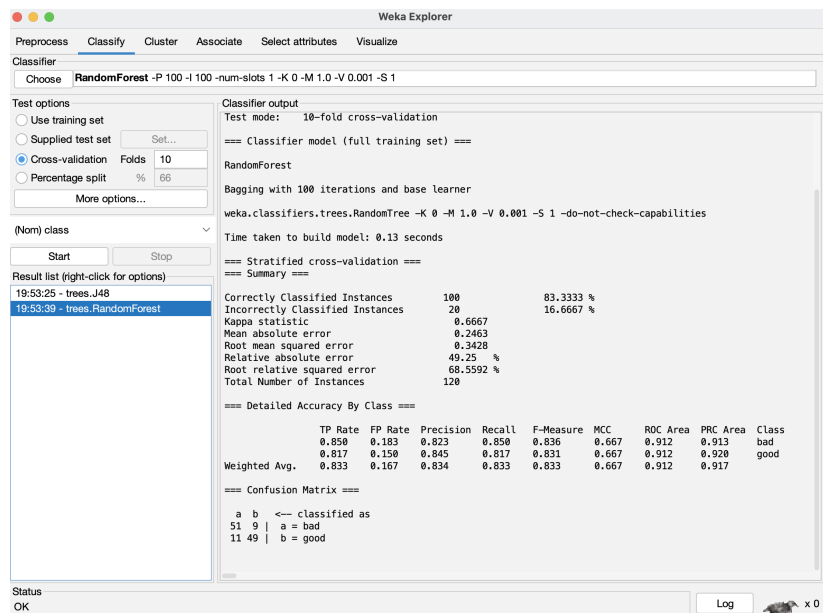


Figure 14: Weka Result using RandomForest model

4.3 Improvements

- Create a sample holder to more effectively assemble the samples on and off for doing experiments, which might also be useful for the CV segmentation.
- Remove the noise in the streaming GUI window caused by the normalization from 16 bit image data.
- Consider to containerize the software working environment into docker or cloud platform since the installation of working environment is very time-consuming.
- Change the current relay module into one with larger capacity tolerance.

4.4 Future Development

Currently, I have developed a reliable software solution for data acquisition and analysis. However, to achieve higher classification accuracy and implement the project in the industry, there are additional steps to take.

We need to purify our collected data. Due to nonuniform heating radiation from random positions of two lamps and the thermal camera's view, the radiation is distributed unevenly. Therefore, we need to develop a calibration method to eliminate this nonuniform distribution.

Furthermore, our machine learning (ML) accuracy is still not satisfactory, and we have not met our pre-set goal. There are two reasons for this. Firstly, we have not collected enough data, and during the seed classification process, I used my own eyes for recognition. This approach may lead to misclassification of damaged seeds as healthy ones. Secondly, the current model and parameters used for training and testing may not be suitable. Thus, we need to conduct additional experiments and develop a more robust model for our research.

5 Conclusion

In conclusion, this project report aimed to demonstrate the feasibility and accuracy of a new method for assessing crop health using thermography. The results of the project demonstrated that there is a significant correlation between a plant's viability and its temperature fluctuations, and that non-destructive and non-invasive thermography can be used as a viable alternative to computed tomography (CT) scanning for assessing crop health.

The design of the project instrument was well-developed, with a mechanical design that utilized 3D printing and a black platform made from HPEC material to ensure accurate data collection. The electrical design included a USB relay module to control the power strip, with 10 AWG wires to handle the current load.

The software development project was challenging, but the team successfully developed a robust and effective software solution that met all research objectives. The data acquisition and analysis were conducted using computer vision and machine learning techniques, with two major case studies consisting of 2 different types of samples arranged in various configurations to obtain meaningful statistics and insights into the thermal activity of the seed samples.

The results of the machine learning analysis using J48 and Random Forest algorithms demonstrated moderate accuracy in classifying seed samples into two classes. However, the team acknowledged the need for further experimentation and evaluation to determine the optimal algorithm for this classification problem.

Future development for this project includes the need to develop a calibration method to eliminate non-uniform distribution of radiation and the need to collect more data for higher classification accuracy. Overall, this project shows great potential to revolutionize the way farmers assess crop health and improve overall crop yields using thermography.

6 Acknowledgement

The author extends heartfelt gratitude to Mr. Alan Zayd Zoubi for his invaluable assistance in the mechanical design and implementation of the system case. Special thanks also go to Mr. Steven Lerch for his dedicated efforts in collecting grapevines and conducting freezing treatment on grape buds for data acquisition. Furthermore, the author acknowledges with deep appreciation the contributions of Drs. Justine Vanden Heuvel and Virginia Moore, who generously provided the biological samples for the case studies.

7 Reference

- Steensland, A., & Zeigler, M. (2018). *2018 Global Agricultural Productivity Report® (GAP Report®)*. Global Harvest Initiative. Retrieved from https://globalagriculturalproductivity.org/wp-content/uploads/2019/01/GHI_2018-GAP-Report_FINAL-10.03.pdf
- Malague, X., & Marinetti, S. (1996). *Pulse phase infrared thermography*. Journal of applied physics, 79(5), 2694-2698.
- Malague, X., Galmiche, F., & Ziadi, A. (2002). *Advances in pulsed phase thermography*. Infrared physics & technology, 43(3-5), 175-181.
- Wu, D. & Sun, D. W. (2013). *Advanced applications of hyperspectral imaging technology for food quality and safety analysis and assessment: A review - part ii: Applications*. Innovative Food Science & Emerging Technologies 19, 15–28.
- He, Y., Xiao, Q., Bai, X., Zhou, L., Liu, F., & Zhang, C. (2022). *Recent progress of nondestructive techniques for fruits damage inspection: a review*. Critical Reviews in Food Science and Nutrition, 62(20), 5476-5494.
- Kuzy, J., Jiang, Y., & Li, C. (2018). *Blueberry bruise detection by pulsed thermographic imaging*. Postharvest Biology and Technology, 136, 166-177. Retrieved from <https://www.sciencedirect.com/science/article/abs/pii/S0925521417310682>
- Jiang, Y., Li, C., & Takeda, F. (2016). *Nondestructive detection and quantification of blueberry bruising using near-infrared (NIR) hyperspectral reflectance imaging*. Scientific Reports, 6(1), 35679.

8 Appendix

Code for the project:

https://github.com/gzhai5/Thermography_for_Grape_Mortality

Relay Module Datasheet:

<https://cdn-shop.adafruit.com/product-files/2935/P2935B%20datasheet.pdf>

Relay Module Connection Guide:

<https://www.circuitbasics.com/setting-up-a-5v-relay-on-the-arduino/>

FLIR Spinnaker SDK documentation:

<http://softwareservices.flir.com/Spinnaker/latest/index.html>

Tutorial of how to display opencv video in pyQt app:

<https://gist.github.com/docPhil99/ca4da12c9d6f29b9cea137b617c7b8b1>